complexes, and Table III showing kinetic data of Cr(II) reductions of complexes I–IV (5 pages). Ordering information is given on any current masthead page.

References and Notes

(1) H. Spiecker and K. Wieghardt, *Inorg. Chem.*, **16**, 1290 (1977).
(2) S. Gabriel and J. Colman, *Ber. Dtsch. Chem. Ges.*, **32**, 1536 (1899).
(3) S. Gabriel and J. Colman, *Ber. Dtsch. Chem. Ges.*, **37**, 3649 (1904).
(4) (a) J. Tafel and E. Enoch, *Ber. Dtsch. Chem. Ges.*, **23**, 103 (1890); (b) S. Gabriel and J. Colman, *ibid.*, **32**, 1524 (1899).
(5) A. Ladenburg and K. Scholtze, *Ber. Dtsch. Chem. Ges.*, **33**, 1081 (1900).
(6) K. Wieghardt, *J. Chem. Soc., Dalton Trans.*, 2538 (1973).
(7) G. Maas, *Z. Anorg. Allg. Chem.*, **432**, 203 (1977).
(8) A detailed discussion of this point is given in ref 1.
(9) (a) J. C. Chen and E. S. Gould, *J. Am. Chem. Soc.*, **95**, 5544 (1973); (b) I. Baldea, K. Wieghardt, and A. G. Sykes, *J. Chem. Soc., Dalton Trans.*, 78 (1977).
(10) H. Spiecker and K. Wieghardt, *Inorg. Chem.*, **15**, 909 (1976).

Contribution from Physikalisches Institut and Institut für Physikalische Chemie, Universität Erlangen-Nürnberg, D-8520 Erlangen, West Germany, and the School of Chemistry, University of New South Wales, Kensington, New South Wales, Australia 2033

The High-Spin ($^5T_2$) ⇌ Low-Spin ($^1A_1$) Transition in Solid Bis[2-(2-pyridylamino)-4-(2-pyridyl)thiazole]iron(II) Dinitrate. Its Dependence on Time and on the Previous History of the Specimen

G. RITTER,[1a] E. KÖNIG,*[1b] W. IRLER,[1a] and H. A. GOODWIN[2]

Received April 6, 1977

The continuous high-spin ($^5T_2$) ⇌ low-spin ($^1A_1$) transition in ^{57}Fe-enriched (>90%) solid $[Fe(paptH)_2](NO_3)_2$ (paptH = 2-(2-pyridylamino)-4-(2-pyridyl)thiazole) has been studied in detail by Mössbauer spectroscopy. When the sample is cooled slowly, the transition is almost complete, the $^5T_2$ fraction at 290 and 105 K being >0.95 and 0.067, respectively. A pronounced hysteresis of $\Delta T_c = 34$ K has been observed, the transition being centered at $T_C^{>} = 263$ K for increasing temperature and at $T_C^{<} = 229$ K for decreasing temperature. When the sample is cooled rapidly, a considerable fraction (~0.40) of the $^5T_2$ state molecules is metastable at 105 K. Subsequent heating causes a high-spin ($^5T_2$) → low-spin ($^1A_1$) transformation to the "equilibrium" composition. The kinetics of this transformation were studied at 160, 170, and 180 K. The resulting mean lifetimes for the $^5T_2$ state are, serially, τ = 14460, 5590, and 1160 s. The activation energy for the process is ΔE = 7.5 kcal mol^{-1}. Various other high-spin ($^5T_2$) ⇌ low-spin ($^1A_1$) systems have been studied for similar nonequilibrium behavior with negative results.

Introduction

It has been suggested previously[3] that, on the basis of magnetic susceptibilities between about 80 and 380 K and visual color changes, several iron(II) complexes of the tridentate ligand 2-(2-pyridylamino)-4-(2-pyridyl)thiazole (abbreviated paptH) exhibit high-spin ($^5T_2$) ⇌ low-spin ($^1A_1$) transitions as solids. This inference has recently been confirmed[4] by ^{57}Fe Mössbauer-effect studies on absorbers enriched to >90% ^{57}Fe of $[Fe(paptH)_2]X_2 \cdot H_2O$, where X = NO_3 and ClO_4. As in several other $[Fe^{II}–N_6]$ systems studied previously,[5–8] the high-spin ($^5T_2$) ⇌ low-spin ($^1A_1$) transition in these complexes extends over a considerable range of temperature and is incomplete at cryogenic temperatures.

In the course of the initial studies,[3] a marked time dependence of the magnetism of $[Fe(paptH)_2](NO_3)_2$ was noted, the origin of which having been attributed to a slow phase change accompanying the change from high-spin ($^5T_2$) to low-spin ($^1A_1$) ground state. If confirmed, this observation might prove to be of importance with respect to the mechanism of high-spin ($^5T_2$) ⇌ low-spin ($^1A_1$) transitions in solid iron(II) complexes. Therefore, in the present study, we report the results of a detailed investigation, by the ^{57}Fe Mössbauer effect, of the dependence of the high-spin ($^5T_2$) ⇌ low-spin ($^1A_1$) transition in enriched absorbers of $[Fe(paptH)_2](NO_3)_2$ on both time and the previous history of the specimen.

Experimental Section

The sample of $[Fe(paptH)_2](NO_3)_2$ was prepared as described elsewhere,[3] employing iron metal enriched to >90% in ^{57}Fe as the starting material. The homogeneity and purity of the product were verified by chemical analyses, magnetism, and the Mössbauer spectra reported below.

Mössbauer spectra were measured with a spectrometer of the constant-acceleration type (Frieseke und Hoepfner FHT 800A), operating in the multiscaler mode. The absorber was of polycrystalline form and contained 0.63 mg/cm^2 of ^{57}Fe. A 50 mCi source of ^{57}Co in rhodium was used, the calibration being effected with a metallic-iron absorber. All velocity scales and isomer shifts are referred to the iron standard at 298 K. To convert to the sodium nitroprusside scale add +0.257 mm s^{-1}. Movement of the source toward the absorber corresponds to positive velocities. Variable-temperature measurements between 105 and 290 K were obtained by the use of a small heating coil with the sample placed in a superinsulated cryostat. The temperatures were carefully monitored by means of a calibrated copper/constantan thermocouple, a cryogenic temperature controller (Artronix Model 5301-E), and liquid nitrogen as coolant. In order to determine reliable values for the effective thickness, all measurements were performed with the identical geometrical arrangement for source, absorber, and detector. The resulting data were carefully corrected for nonresonant background of the γ rays and computer-fitted to Lorentzian line shapes. The utilization of a sample enriched in ^{57}Fe allowed the relatively rapid accumulation of spectra, and hence measurement of the time dependence of the spectral characteristics became feasible. The quality of the measurements is demonstrated in Figure 1, in which the diagram on the left (a) shows a spectrum accumulated within 15 min, whereas the diagram on the right (b) shows data collected over a period of 60 min. Here the vertical bars indicate the magnitude of the statistical error. Evidently, the spectrum displayed on the left (a) is sufficiently accurate for the present purposes.

To obtain values of the effective thickness $t_{^5T_2}$ and $t_{^1A_1}$, the well-known area method[9,10] has been used. In the Mössbauer spectrum of an absorber of finite thickness, the normalized area[10] for the ith line is determined by eq 1, provided the lines are well resolved. Here

$$A_i = {}^1/_2 \pi f_S \Gamma_i L(t_i) \tag{1}$$

Γ_i is the line width of the ith absorber line and f_S is the Debye–Waller factor of the source. Also, A_i is independent of the line shape of the source. For a Lorentzian line shape of the absorber line, the saturation function $L(t_i)$ assumes the form[9]

$$L(t_i) = t_i e^{-t_i/2} [I_0(t_i/2) + I_1(t_i/2)] \tag{2}$$

where I_γ are the Bessel functions with an imaginary argument.

In order to determine, from the quantity A_i, the effective thickness t_i, the inverse function $t_i(L)$ is required. This function is given in numerical form by eq 3.[11] For $0 \le t_i \le 8$, the accuracy of eq 3 is

$$t_i(L) = 3.2250L - 8.2620 + (8.9679L^2 - 36.8464L + 68.2803)^{1/2} \tag{3}$$

0020-1669/78/1317-0224$01.00/0

Table I. ^{57}Fe Mössbauer-Effect Data for $[Fe(paptH)_2](NO_3)_2$

T, K	ΔE_Q ($^5T_2$), mm s^{-1}	δ^{IS} ($^5T_2$),[a] mm s^{-1}	ΔE_Q ($^1A_1$), mm s^{-1}	δ^{IS} ($^1A_1$),[a] mm s^{-1}	$t_{^5T_2}/(t_{^5T_2}+t_{^1A_1})$ For falling temp	$t_{^5T_2}/(t_{^5T_2}+t_{^1A_1})$ For rising temp
290	2.41 ± 0.02	+0.93 ± 0.03	~1.25[b]	~0.36[b]	>0.95	>0.95
280	2.43 ± 0.02	+0.93 ± 0.03	1.25 ± 0.03	+0.36 ± 0.04		0.910
270	2.44 ± 0.02	+0.93 ± 0.03	1.26 ± 0.02	+0.36 ± 0.03	0.943	0.810
260	2.45 ± 0.02	+0.93 ± 0.03	1.26 ± 0.02	+0.36 ± 0.03	0.922	0.420
250	2.46 ± 0.02	+0.94 ± 0.03	1.26 ± 0.02	+0.36 ± 0.03	0.882	0.341
240	2.47 ± 0.02	+0.94 ± 0.03	1.27 ± 0.02	+0.37 ± 0.03	0.794	0.273
230	2.48 ± 0.02	+0.94 ± 0.03	1.27 ± 0.02	+0.37 ± 0.03	0.532	0.234
220	2.49 ± 0.02	+0.94 ± 0.03	1.27 ± 0.02	+0.37 ± 0.03	0.326	0.184
210	2.50 ± 0.02	+0.94 ± 0.03	1.27 ± 0.02	+0.37 ± 0.03	0.229	0.164
200	2.51 ± 0.02	+0.94 ± 0.03	1.27 ± 0.02	+0.37 ± 0.03	0.168	
190	2.52 ± 0.02	+0.95 ± 0.03	1.28 ± 0.02	+0.37 ± 0.03	0.129	0.125
170	2.53 ± 0.02	+0.95 ± 0.03	1.28 ± 0.02	+0.36 ± 0.03	0.102	0.107
160	2.53 ± 0.02	+0.95 ± 0.03	1.28 ± 0.02	+0.36 ± 0.03		0.091
150	2.54 ± 0.02	+0.95 ± 0.03	1.28 ± 0.02	+0.36 ± 0.03	0.086	0.089
130	2.55 ± 0.03	+0.95 ± 0.04	1.28 ± 0.02	+0.36 ± 0.03	0.075	0.077
105	2.55 ± 0.03	+0.95 ± 0.04	1.29 ± 0.02	+0.35 ± 0.03	0.067	0.067

[a] Isomer shifts δ^{IS} are listed relative to natural iron at 298 K. [b] Very small fraction of spectrum present. Only approximate values of the Mössbauer parameters can be given.

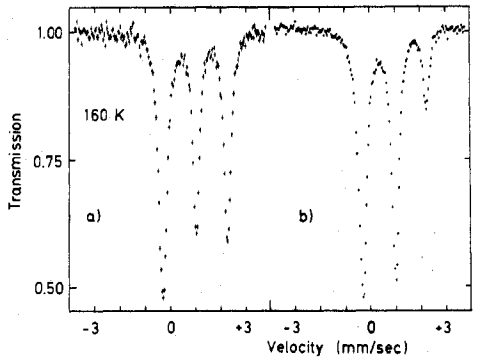

Figure 1. ^{57}Fe Mössbauer spectra of solid $[Fe(paptH)_2](NO_3)_2$ at 160 K. Left spectrum (a) accumulated at $t \sim 0$, within 15 min (i.e., 0–15 min), and right spectrum (b) accumulated at $t \sim 400$ min, within 60 min (i.e., 380–440 min).

better than 1%. In the case considered here, the low-energy lines originating from the $^5T_2$ and the $^1A_1$ quadrupole doublets show complete overlap. Therefore, in our analysis, the high-energy line of the appropriate doublet is employed exclusively. These lines are well resolved. In addition, the powder absorber studied did not show any effects which would produce different areas of the two lines of the same quadrupole doublet (such as, e.g., texture). Consequently, the effective thickness for a single line of the corresponding quadrupole doublet is determined by eq 4. Here, w denotes the number of resonant

$$t^{5}_{T_2} = {}^1/_2 w \sigma_0 f^{5}_{T_2} n^{5}_{T_2}$$
$$t^{1}_{A_1} = {}^1/_2 w \sigma_0 f^{1}_{A_1} (1 - n^{5}_{T_2}) \qquad (4)$$

nuclei per unit area of absorber, σ_0 is the resonant cross section, and $f_{^5T_2}$ and $f_{^1A_1}$ are the Debye–Waller factors of the corresponding ground state. In addition, $n_{^5T_2}$ is the site fraction of molecules in the $^5T_2$ ground state. In a paper by Stone,[12] analytical expressions are given, in terms of the parameters of the absorber, for the parameters of a least-squares Lorentzian which has been fitted to the Mössbauer spectrum for a thick absorber. From Table I of Stone,[12] the ratio

$$\frac{(A_i)_m}{(A_i)_f} = \frac{\text{measured area}}{\text{area of Lorentzian-fit curve}} \qquad (5)$$

may be easily calculated, giving for $t \leq 4$: $1 \geq (A_i)_m/(A_i)_f \geq 0.99$. Therefore, it is, in very good approximation,

$$A_f(^5T_2) = {}^1/_2 \pi f_S \Gamma^{5}_{T_2} L(t_{^5T_2})$$
$$A_f(^1A_1) = {}^1/_2 \pi f_S \Gamma_{^1A_1} L(t_{^1A_1}) \qquad (6)$$

In the present study, it is $\Gamma_{^5T_2} = \Gamma_{^1A_1} = \Gamma_0$, where Γ_0 is the natural

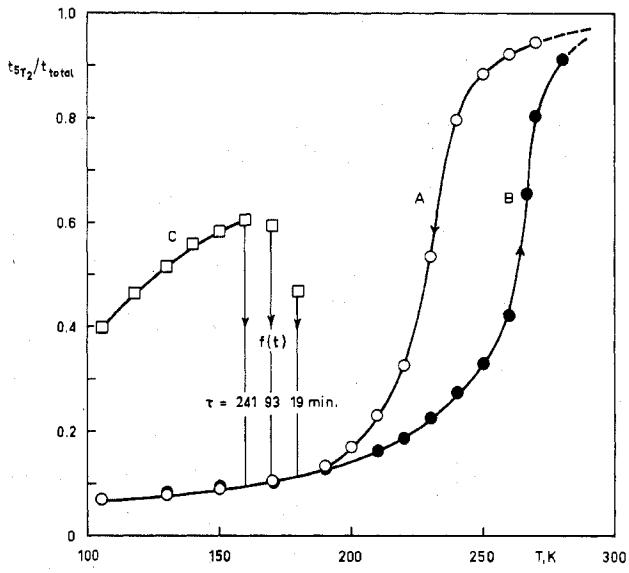

Figure 2. Temperature dependence of the relative effective thickness $t_{^5T_2}/(t_{^5T_2} + t_{^1A_1})$ of $[Fe(paptH)_2](NO_3)_2$ (A) with slowly decreasing temperature followed by (B) increasing temperature; (C) with increasing temperature after the sample had been rapidly cooled in liquid nitrogen.

line width. The factor ${}^1/_2 \pi f_S \Gamma_0$ has been determined by measurements on sodium nitroprusside absorbers of known effective thickness. The determination of $n_{^5T_2}$ and $n_{^1A_1} = 1 - n_{^5T_2}$ is not without difficulties. Because of the possible difference[7,8] between $f_{^5T_2}$ and $f_{^1A_1}$, an observed variation in $t_{^5T_2}$ and $t_{^1A_1}$ will not directly reflect the variation of $n_{^5T_2}$ and $n_{^1A_1}$, respectively. Therefore, values of the relative effective thickness for the $^5T_2$ ground state, viz. $t_{^5T_2}/(t_{^5T_2} + t_{^1A_1})$, are listed in Table I.

Results

At 290 K, the highest temperature studied, the Mössbauer spectrum of $[Fe(paptH)_2](NO_3)_2$ consists to >95% of a single doublet, characterized by the quadrupole splitting $\Delta E_Q = 2.41$ mm s^{-1} and the isomer shift $\delta^{IS} = +0.93$ mm s^{-1} (cf. Figure 2 of our previous study).[4] On the basis of these data, assignment of the doublet to the high-spin $^5T_2$ ($t_2^4e^2$) ground state is justified. Term symbols within cubic symmetry are employed for convenience only. A second weak doublet (<5%) characterized by $\Delta E_Q = 1.25$ mm s^{-1} and $\delta^{IS} = +0.36$ mm s^{-1} has been assigned to the ground state $^1A_1$ (t_2^6). In the following, we consider initially the changes in the Mössbauer spectrum which are observed if the temperature is *lowered*

slowly. In this case, the intensity of the $^5T_2$ spectrum decreases as indicated by the values of $t_{^5T_2}/(t_{^5T_2} + t_{^1A_1})$ in column 6 of Table I (also, cf. Figure 2, curve A). Simultaneously, the intensity of the $^1A_1$ spectrum is increasing at the same rate. Finally, at 105 K, the spectrum is for the largest part (i.e., 93.3%) due to the $^1A_1$ doublet, the corresponding Mössbauer parameters being given by $\Delta E_Q = 1.29$ mm s^{-1} and $\delta^{IS} = +0.35$ mm s^{-1}. If the temperature is now *slowly increased*, spectra which are similar, on a qualitative basis, to those discussed above are obtained in reversed order. It should be noted, however, that considerably different values of $t_{^5T_2}/(t_{^5T_2} + t_{^1A_1})$ result if spectra at the same temperature are compared (cf. columns 6 and 7 of Table I). For convenience of presentation we define a transition temperature, T_C, as that temperature at which the $^5T_2$ fraction becomes 50%. From Figure 2 it is then evident that the high-spin ($^5T_2$) $\rightleftharpoons$ low-spin ($^1A_1$) transition is centered, for decreasing temperature, on $T_C^< = 229$ K, whereas for increasing temperature one obtains $T_C^> = 263$ K. The transition in $[Fe(paptH)_2](NO_3)_2$ is thus associated with a hysteresis of $\Delta T_C = 34$ K. Only one detailed study of hysteresis effects at a high-spin ($^5T_2$) $\rightleftharpoons$ low-spin ($^1A_1$) transition seems to have been reported,[13] and this is concerned with the cooperative transition in $[Fe(4,7\text{-}(CH_3)_2phen)_2(NCS)_2]$. In the latter case, the transition is completed within 2 K,[14] the thermodynamic theory of Slichter and Drickamer[15] having been found to be only in qualitative agreement with the measurements. In $[Fe(paptH)_2](NO_3)_2$, the transition takes place over ~100 K and, consequently, the above theory[15] was found to be completely inadequate.

A rather different behavior is encountered if, starting from 290 K, the temperature is lowered *rapidly*, e.g., by immersion of the absorber in liquid nitrogen. In this case, a Mössbauer spectrum characterized by $t_{^5T_2}/(t_{^5T_2} + t_{^1A_1}) = 0.39$ is obtained at 105 K, the individual Mössbauer parameters, i.e., ΔE_Q and δ^{IS}, for the $^5T_2$ and $^1A_1$ ground states being identical with those obtained for slow cooling; cf. Table I. If the temperature of the absorber is now slowly raised, increasing values of $t_{^5T_2}/(t_{^5T_2} + t_{^1A_1})$ result, cf., e.g., 0.462 for 118 K, 0.560 for 140 K, and 0.605 for 160 K (viz. Figure 2, curve C). At 160 K a slow transformation of the high-spin ($^5T_2$) ground state into the low-spin ($^1A_1$) ground state is observed. This time dependence of the spectrum is characterized by a mean lifetime of the $^5T_2$ ground state, τ, of 241 min, similar results being obtained at 170 and 180 K. These observations are summarized in the schematic of Figure 2. Evidently, the starting points in Figure 2 for the temperatures of 170 and 180 K are inaccurate, due to progress of the high-spin ($^5T_2$) → low-spin ($^1A_1$) transformation. Also, measurements of the time dependence above 180 K are not practicable, due to the low mean lifetime of the metastable $^5T_2$ ground-state molecules. On the other hand, the extrapolated value of the mean lifetime at 145 K is τ ~3060 min, and indeed two measurements within a time interval of 630 min produced $(t_{^5T_2} - t^{\infty}{}_{^5T_2})/(t^0{}_{^5T_2} - t^{\infty}{}_{^5T_2}) = 0.83$, whereas from $\tau = 3060$ min this ratio follows as 0.814. The spectra which result if the transformation comes to completion are identical with those obtained for the same temperature with slow cooling (cf. Table I and above).

The above results may be employed to investigate the kinetics of the high-spin ($^5T_2$) → low-spin ($^1A_1$) transformation in solid $[Fe(paptH)_2](NO_3)_2$. If the observed transformation is of first order, the rate law will be given by eq 7. Here, $t^0{}_{^5T_2}$

$$t_{^5T_2} - t^{\infty}{}_{^5T_2} = (t^0{}_{^5T_2} - t^{\infty}{}_{^5T_2})e^{-t/\tau} \quad (7)$$

and $t^{\infty}{}_{^5T_2}$ are the initial and final values of $t_{^5T_2}$, respectively, and t is the time and τ is the mean lifetime of the $^5T_2$ ground state. As a consequence of the definition of the effective thickness $t_{^5T_2}$ (cf. eq 4), this relation reflects directly the behavior of the site fraction $n_{^5T_2}$. The spectrum of the sample

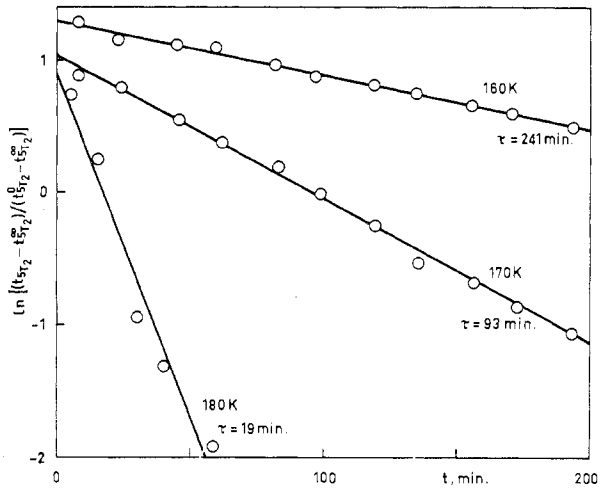

Figure 3. Dependence of $\ln [(t_{^5T_2} - t^{\infty}{}_{^5T_2})/(t^0{}_{^5T_2} - t^{\infty}{}_{^5T_2})]$ on time for the high-spin ($^5T_2$) → low-spin ($^1A_1$) transformation in quenched-in $[Fe(paptH)_2](NO_3)_2$ at 160, 170, and 180 K.

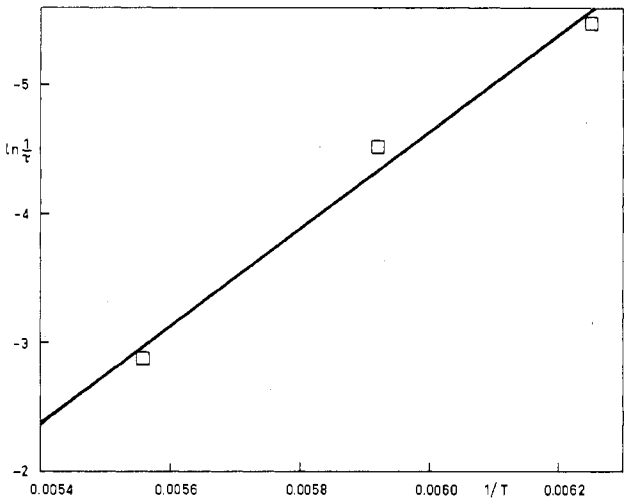

Figure 4. Arrhenius plot for the high-spin ($^5T_2$) → low-spin ($^1A_1$) transformation in quenched-in $[Fe(paptH)_2](NO_3)_2$.

Table II. Kinetic Parameters for the High-Spin ($^5T_2$) → Low-Spin ($^1A_1$) Transformation in $[Fe(paptH)_2](NO_3)_2$

T, K	$10^{-3}\tau$, s	k, s^{-1}
160	14.46	6.92
170	5.59	17.9
180	1.16	85.9

was collected at regular time intervals at temperatures of 160, 170, and 180 K, and the results are incorporated into Figure 3, in which $\ln [(t_{^5T_2} - t^{\infty}{}_{^5T_2})/(t^0{}_{^5T_2} - t^{\infty}{}_{^5T_2})]$ is plotted as a function of time, t. The values of t in Figure 3 have been taken at the midpoint of the time interval required for the measurement. This method provides the exact results for the mean lifetime, τ. The resulting linear plots are evidence for the applicability of eq 4, the slopes giving values of τ for the temperatures employed. The values of the rate constants $k = 1/\tau$, as well as the mean lifetimes τ, have been collected in Table II. Figure 4 shows the Arrhenius plot corresponding to eq 8, which is obtained from the data of Table II. The

$$\ln \frac{1}{\tau} = -\frac{\Delta E}{kT} + \ln A \quad (8)$$

activation energy of the transformation follows according to eq 8 as $\Delta E = 7.5 \pm 1.8$ kcal mol^{-1}, whereas the frequency factor is given by $A = 6.4 \times 10^7$. If the relation between A and the activation entropy S^* (eq 9) is utilized, the result for

$$A = (2.058 \times 10^{10}) T e^{S^{\ddagger}/R} \quad (9)$$

160 K is $S^{\ddagger} = -21.56$ cal K^{-1} mol^{-1}, which is well within the expected range.

Discussion

The observation that a pronounced thermal hysteresis is associated with the high-spin ($^5T_2$) ⇌ low-spin ($^1A_1$) transition in $[Fe(paptH)_2](NO_3)_2$ is of considerable interest. Recently, hysteresis effects have been found for cooperative (i.e., discontinuous) high-spin ($^5T_2$) ⇌ low-spin ($^1A_1$) transitions in $[Fe(4,7\text{-}(CH_3)_2phen)_2(NCS)_2]$,[13] where phen = 1,10-phenanthroline, and $[Fe(2\text{-pic})_3]Cl_2 \cdot H_2O$,[16] where 2-pic = 2-aminomethylpyridine. This phenomenon has indeed been expected on the basis of a thermodynamic description of high-spin ⇌ low-spin transitions.[15] We have shown elsewhere[17] that thermal hysteresis may be understood as well if a statistical model inclusive of lattice vibrations is applied. The present results demonstrate that a high-spin ⇌ low-spin system may remain metastable in a local free-energy minimum, even if the transition is of the continuous type.[18] Apparently, the high-spin ($^5T_2$) ⇌ low-spin ($^1A_1$) transition in $[Fe(paptH)_2](NO_3)_2$ involves a phase change despite its completely continuous appearance. This presumes the generation of domains, possibly by both $^5T_2$ and $^1A_1$ molecules, and a transformation via hybrid crystal formation. The free energy will then contain an additional term ξ, comprising either the compression or the tension energy.[19] Suppose that the system contains a fraction $n_{^5T_2}$ of the high-spin ($^5T_2$) molecules and a fraction $1 - n_{^5T_2}$ of the low-spin ($^1A_1$) molecules. The term ξ will then be different for the transformation $^1A_1 \rightarrow {}^5T_2$ and $^5T_2 \rightarrow {}^1A_1$; i.e., $\xi_{^1A_1{}^5T_2} \neq \xi_{^5T_2{}^1A_1}$. If the specific volumes of low-spin and high-spin molecules are different and, presumably, in the present case $V_{^5T_2} > V_{^1A_1}$,[20,21] domains of high-spin molecules formed within a crystal of the low-spin phase will experience a compression, while domains of low-spin molecules formed within the high-spin phase will be in tension.[22] The hysteresis observed for the system studied here is tentatively attributed to this effect. It should be noted that the normal mode of transformation will involve nucleation.[22] In the present system, the variation of $t_{^5T_2}/(t_{^5T_2} + t_{^1A_1})$ is shifted higher and lower for raising and for lowering of temperature, respectively (cf. Figure 2). In the former case, nucleation of $^5T_2$ molecules will be of prime importance, and the transition thus arises only for sufficiently large superheating. In the latter case, the transition occurs by nucleation of $^1A_1$ molecules, and thus considerable supercooling is required.

The dependence of the Mössbauer spectrum of $[Fe(paptH)_2](NO_3)_2$ on the rate of cooling is demonstrated in Figure 5. The spectrum at the top of Figure 5 has been obtained by slow cooling to 105 K and corresponds to the data listed in Table I. The bottom spectrum results by fast cooling in liquid nitrogen and corresponds to the point on curve C of Figure 2 at 105 K. The spectrum in the center of Figure 5 has been obtained by cooling within a few minutes and shows an intermediate value of $t_{^5T_2}/(t_{^5T_2} + t_{^1A_1})$. It is evident that low-temperature Mössbauer spectra of $[Fe(paptH)_2](NO_3)_2$ are significantly dependent on the previous history of the specimen.

The quenching-in of high-spin ($^5T_2$) molecules of solid $[Fe(paptH)_2](NO_3)_2$ by fast cooling from 290 to 105 K is not completely unexpected if the high-spin ($^5T_2$) → low-spin ($^1A_1$) transformation is not extremely fast. At first sight surprising is the increasing character of $t_{^5T_2}/(t_{^5T_2} + t_{^1A_1})$, which is found if the temperature of the sample is subsequently raised (cf. Figure 2, curve C). This behavior may be rationalized by assuming that, in the temperature range 105–160 K, the low-spin ($^1A_1$) → high-spin ($^5T_2$) transformation is effective, although its rate is governed by the fraction of available $^5T_2$ molecules. Since $n_{^5T_2} \sim 0.4$ (105 K) for the quenched-in system, the transformation proceeds to form additional $^5T_2$ molecules, whereas in the equilibrium system $n_{^5T_2} \sim 0.07$ (105 K) and, consequently, the $^5T_2$ formation is proceeding to a much lesser degree. It should be noted that the assumption introduced here is in line with the recently observed domain formation in $[Fe(4\text{-}CH_3phen)_2(NCS)_2]$,[23,24] although nonequilibrium behavior has not been detected in this case.

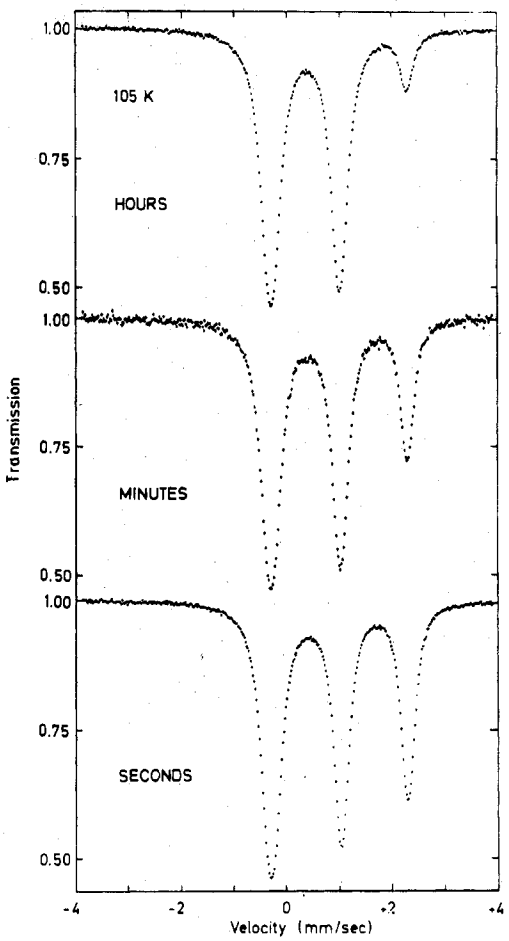

Figure 5. Dependence of the ^{57}Fe Mössbauer spectrum of $[Fe(paptH)_2](NO_3)_2$ at 105 K on the rate of cooling: upper spectrum for slow cooling (h), central spectrum for reasonably fast cooling (min), and bottom spectrum for very fast cooling (s).

Various additional systems showing high-spin ($^5T_2$) ⇌ low-spin ($^1A_1$) transitions have been investigated for nonequilibrium behavior at low temperatures by fast cooling of samples in liquid nitrogen. The systems studied are the following: $[Fe(bpy)_2(NCS)_2]$ polymorph(III)[25] $[Fe(2\text{-}CH_3phen)_3](BF_4)_2$,[5] $[Fe(pythiaz)_2](BF_4)_2$,[7] $[Fe(papt)_2]$ sample B,[8] $[Fe(papt)_2]\cdot{}^4/_3CHCl_3$,[8] and $[Fe(4,7\text{-}(CH_3)_2phen)_2(NCS)_2]$.[14] For each of these systems the spectra obtained at 105 K for samples cooled rapidly and slowly from 290 K were identical.

In $[Fe(paptH)_2](NO_3)_2$, the high-spin ($^5T_2$) → low-spin ($^1A_1$) transformation which is responsible for the establishment of equilibrium thus seems to proceed with a reasonably fast rate only at temperatures above 150 K. The rates at 160, 170, and 180 K are in a convenient region to be studied by Mössbauer spectroscopy, and thus the results quoted above were obtained. At $T \geq 200$ K, this transformation is always very fast, and consequently, nonequilibrium high-spin ($^5T_2$) fractions are not observed. On the other hand, extrapolation to 105 K produces $\tau \sim 10^7$ min, which demonstrates why $^5T_2$ molecules quenched-in at this temperature are metastable when once formed.

The present results are not completely consistent with the time dependence previously reported[3] for the magnetic susceptibility of $[Fe(paptH)_2](NO_3)_2$. Although the origin of this discrepancy is not obvious at this moment, the lower accuracy of magnetic measurements with the Gouy method, possible differences between different samples and differences in the rate of cooling for the Mössbauer and magnetic measurements have to be considered.

Obviously, the high-spin → low-spin and low-spin → high-spin transformations will be present in all solid systems showing high-spin, low-spin transitions. Apparent equilibrium behavior will be found where both transformations are reasonably fast. The present system is unique in that the rates are such that, at least in part, a detailed observation of these processes is possible.

Acknowledgment. The authors appreciate financial support by the Deutsche Forschungsgemeinschaft and the Fonds der Chemischen Industrie. The comments of one referee are particularly acknowledged, since they were helpful in improving the quality of presentation.

Registry No. $[Fe(paptH)_2](NO_3)_2$, 15229-01-3.

References and Notes

(1) (a) Physikalisches Institut, Universität Erlangen-Nürnberg. (b) Institut für Physikalische Chemie, Universität Erlangen-Nürnberg.
(2) School of Chemistry, University of New South Wales.
(3) R. N. Sylva and H. A. Goodwin, *Aust. J. Chem.*, **20**, 479 (1967).
(4) E. König, G. Ritter, and H. A. Goodwin, *Chem. Phys. Lett.*, **44**, 100 (1976).
(5) E. König, G. Ritter, H. Spiering, S. Kremer, K. Madeja, and A. Rosenkranz, *J. Chem. Phys.*, **56**, 3139 (1972).
(6) E. König, G. Ritter, B. Braunecker, K. Madeja, H. A. Goodwin, and F. E. Smith, *Ber. Bunsenges. Phys. Chem.*, **76**, 393 (1972).
(7) E. König, G. Ritter, and H. A. Goodwin, *Chem. Phys.*, **1**, 17 (1973).
(8) E. König, G. Ritter, and H. A. Goodwin, *Chem. Phys.*, **5**, 211 (1974).
(9) G. A. Bykov and Pham Zuy Hien, *Zh. Eksp. Teor. Fiz.*, **43**, 909 (1962).
(10) G. Lang, *Nucl. Instrum. Methods*, **24**, 425 (1963).
(11) H. Spiering and H. Vogel, *Hyperfine Interact.*, **3**, 221 (1977).
(12) A. J. Stone, *Nucl. Instrum. Methods*, **107**, 285 (1973).
(13) E. König and G. Ritter, *Solid State Commun.*, **18**, 279 (1976).
(14) E. König, G. Ritter, and B. Kanellakopulos, *J. Phys. C*, **7**, 2681 (1974).
(15) C. P. Slichter and H. G. Drickamer, *J. Chem. Phys.*, **59**, 2142 (1972).
(16) M. Sorai, J. Ensling, K. M. Hasselbach, and P. Gütlich, *Chem. Phys.*, **20**, 197 (1977).
(17) R. Zimmermann and E. König, *J. Phys. Chem. Solids*, **38**, 779 (1977).
(18) E. König and G. Ritter, *Mössbauer Eff. Methodol.*, **9**, 1 (1974).
(19) A. R. Ubbelohde, *Z. Phys. Chem. (Frankfurt am Main)*, **37**, 183 (1963).
(20) E. König and K. J. Watson, *Chem. Phys. Lett.*, **6**, 457 (1970).
(21) M. A. Hoselton, L. J. Wilson, and R. S. Drago, *J. Am. Chem. Soc.*, **97**, 1722 (1975).
(22) A. R. Ubbelohde, *J. Chim. Phys. Phys.-Chim. Biol.*, **62**, 33 (1966).
(23) E. König, G. Ritter, W. Irler, and B. Kanellakopulos, *J. Phys. C*, **10**, 603 (1977).
(24) B. Kanellakopulos, E. König, G. Ritter, and W. Irler, *J. Phys. (Paris), Suppl.*, **37**, C6-459 (1976).
(25) E. König, K. Madeja, and K. J. Watson, *J. Am. Chem. Soc.*, **90**, 1146 (1968).

Contribution from the Department of Chemistry, University of New Orleans, New Orleans, Louisiana 70122

Solvent and Substituent Effects on the Electron-Transfer Rate Constants of Tetraphenylporphyrins and Their Iron Complexes

SEBRINA NI, L. DICKENS, J. TAPPAN, L. CONSTANT, and D. G. DAVIS*

Received June 16, 1977

The effect of substituents on the heterogeneous electron-transfer rates of para- and meta-substituted tetraphenylporphyrins and iron tetraphenylporphyrins was investigated by cyclic voltammetry. In all cases electron-donating substituents caused cathodic shifts in the half-wave potential, $E_{1/2}$, and a relationship between $E_{1/2}$ and the Hammett constant σ was found. The heterogeneous rate of electron transfer in dimethyl sulfoxide (Me_2SO) and dimethylacetamide (DMA) showed some relationship with σ, but it appears that solvent effects are more important than previously reported. Metal-free porphyrins were studied in butyronitrile (*n*-PrCN) and when compared with previous studies indicated a higher degree of susceptibility to electron-withdrawing effects for the first ring reduction than for the iron porphyrins.

Introduction

Investigation of the electron-transfer reactions of iron porphyrins is of great interest because of their importance as biological electron-transfer agents.[1] Although iron porphyrins may be oxidized in at least two one-electron steps in aprotic media,[2,3] we shall concentrate here on the three possible one-electron reduction steps[4,5] due to solvent limitations. A number of studies have shown that their reduction potentials and rate of heterogeneous electron transfer depend on solvent medium and axialy coordinated ligands,[6-8] as well as porphyrin basicity. Recently, correlations between chemical and physical properties and porphyrin ring substituents have appeared. Substituent effects on electronic spectra,[10] equilibrium constants for the addition of axial ligands to metalloporphyrins,[11-15] and potentials for porphyrin redox reactions have been studied.[14,16-18]

Previous reports have quantified the effect of substituents on the oxidation and reduction potentials of transition-metal complexes,[14,16] including those of meta- and para-substituted iron porphyrins.[19] Here we wish to extend the work to the heterogeneous electron-transfer rate constants, k_o's, in different solvents and to rate measurements on metal-free porphyrins.

The electrode reactions investigated here include reactions 1–5. P is (*p*-x)TPP^{2-} or (*m*-x)TPP^{2-}, TPP^{2-} represents tetraphenylporphyrin, and x is an electron-withdrawing or -donating group placed in the para or meta positions of the four phenyl rings of TPP^{2-}.

$$[Fe^{III}P]^+ + e^- = [Fe^{II}P]^0 \quad (1)$$

$$[Fe^{II}P]^0 + e^- = [Fe^{I}P]^- \quad (2)$$

$$[Fe^{I}P]^- + e^- = [FeP]^{2-} \quad (3)$$

$$[H_2P]^0 + e^- = [H_2P]^- \quad (4)$$

$$[H_2P]^- + e^- = [H_2P]^{2-} \quad (5)$$

The Hammett free energy equation (eq 6)[20] describes

$$\Delta E_{1/2} = 4\sigma\rho \quad (6)$$

half-wave potential changes with different substituents. Rate constant ratios can also be substituted for $\Delta E_{1/2}$'s,[20] and σ values are taken from ref 20.

0020-1669/78/1317-0228$01.00/0